Temperature dependence of the electronic structure of two-dimensional Na gas on the Si(111)-7 × 7 surface

2013 J. Phys.: Condens. Matter 25 305004

(http://iopscience.iop.org/0953-8984/25/30/305004)

J. Phys.: Condens. Matter **25** (2013) 305004 (6pp) doi:10.1088/0953-8984/25/30/305004

Temperature dependence of the electronic structure of two-dimensional Na gas on the Si(111)-7 × 7 surface

H-C Shin[1], J T Seo[1], H W Yeom[2] and J R Ahn[1,3]

[1] Department of Physics, Sungkyunkwan University, Suwon 440-746, Republic of Korea
[2] Center for Low Dimensional Electronic Symmetry and Department of Physics, Pohang University of Science and Technology, Pohang 790-784, Republic of Korea
[3] Department of Physics and SAINT and Center for Integrated Nanostructure Physics (CINAP), Institute for Basic Science (IBS), Sungkyunkwan University, Suwon 440-746, Republic of Korea

E-mail: yeom@postech.ac.kr and jrahn@skku.edu

Received 3 April 2013, in final form 10 June 2013
Published 9 July 2013
Online at stacks.iop.org/JPhysCM/25/305004

Abstract
The temperature dependence of the irreversible phase transition from a two-dimensional gas to an ordered zero-dimensional solid on the Si(111)-7 × 7 surface was studied using photoemission spectroscopy. With increasing Na coverage, the two-dimensional Na gas, which is a state of highly mobile Na atoms, undergoes a phase transition into ordered zero-dimensional magic nanoclusters at room temperature. The critical Na coverage of the phase transition was found to increase with reduced temperature. This was used to develop a gas–solid phase diagram of Na atoms on the Si(111)-7 × 7 surface as a function of Na coverage and sample temperature based on the electronic structure. The temperature dependence of the phase transition can be ascribed to the suppression of the thermal energy that is required to overcome the energetic barrier between the two-dimensional gas and the zero-dimensional solid at low temperature, where three different hopping mechanisms are related to the phase transition.

(Some figures may appear in colour only in the online journal)

1. Introduction

Flat and vicinal Si(111) surfaces have been used as atomic templates to grow one-dimensional (1D) atomic structures [1–7] or two-dimensional (2D) arrays of zero-dimensional atomic structures [8–13]. Recently, interesting 1D atomic structures have been grown on vicinal Si(111) surfaces, where 1D charge density waves, 1D spin ordering, and 1D diffusion have been found [1, 4, 6, 7]. On a flat Si(111) surface, the 7 × 7 superstructure of the reconstructed Si(111) surface has been used to grow 2D arrays of magic nanoclusters [8–10, 12–14]. The formation of the magic nanoclusters is not limited to a specific metal atom and various metal atoms have been reported to form magic nanoclusters [8]. A magic nanocluster with six metal atoms is grown on the unfaulted half unit cell in the initial growth stage. After most of the unfaulted half unit cell is covered by the magic nanoclusters, magic nanoclusters begin to form on the faulted half unit cells [8]. Among various magic nanoclusters, Na magic nanoclusters are very unique; other magic nanoclusters form from the initial growth stage, but sodium atoms exist in the form of a gas phase before the magic nanoclusters begin to be assembled [9]. The Na gas–nanocluster phase transition, which was found by STM experiments [9], contributes to the explanation of various experimental results for alkali-metal-covered Si surfaces [15–25]. In particular, the typical surface work function change as a function of alkali-metal coverage was successfully described in terms of the gas–nanocluster phase transitions [9]. Photoemission spectroscopy (PES) experiments demonstrated the existence of surface states corresponding to the Na gas phase and magic nanoclusters

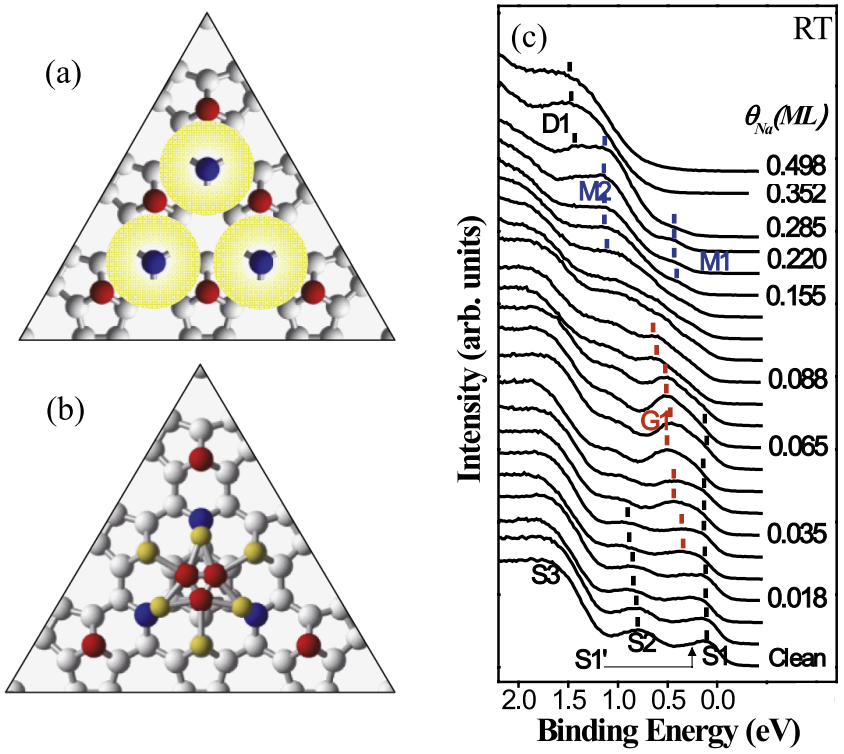

Figure 1. (a) The atomic structure of the Si(111)-7 × 7 surface, where the red and blue spheres denote Si adatoms and restatoms, respectively, and the yellow circles denote basins. (b) The atomic structure of the Na magic nanocluster, where the yellow spheres denote Na atoms. (c) Changes in the PES spectra with increasing θ_{Na} at RT.

at room temperature (RT) [26]. The PES experiments further suggested that the binding energy of the surface state of the Na gas phase changes with increasing Na coverage (θ_{Na}). Scanning tunneling microscopy (STM) experiments demonstrated that Na magic nanoclusters can also be produced when Na atoms are adsorbed below RT. The Na magic nanoclusters, which were observed below RT, were explained by the temperature dependence of the hopping mechanism of Na atoms [27]. However, the temperature dependence of the unique Na gas–nanocluster phase transition has not been clearly understood.

Here, we report the temperature dependence of the Na gas–nanocluster phase transition based on the electronic structure measured using PES experiments. At RT, the surface state of the Na gas phase with a binding energy of 0.6 eV was distinctively different from those of sodium nanoclusters with binding energies of 1.1 and 0.45 eV, respectively, where the critical θ_{Na} of the Na gas–nanocluster phase transition was 0.08 monolayer (ML) [26]. Above 0.22 ML, the 2D array of the magic nanocluster changed into a disordered phase [26]. Na atoms were adsorbed at lower temperatures and the critical θ_{Na} of the gas–nanocluster phase transition was determined from the changes in the surface states. The critical θ_{Na} increased with reduced temperature and the gas–nanocluster phase transition was observed down to 200 K. In contrast, the critical θ_{Na} of the phase transition from the 2D array of nanoclusters to the disordered phase was not changed. Below 200 K, the Na gas phase was directly changed into the disordered phase without the formation of Na magic clusters.

2. Methods

PES measurements were performed using a high resolution angle-resolved electron analyzer (SES-100, Gamma Data) and He I radiation ($h\nu = 21.2$ eV). The nominal energy and angular resolution were better than 13 meV and 0.2°, respectively. Na atoms were deposited using a Na dispenser. The evaporation rate was fixed at 0.022 ML min^{-1} to maintain the growth conditions as close as possible to the previous STM and PES experiments [26, 27]. The relative θ_{Na} was calibrated from the well-established work function changes as measured from the secondary electron cutoff in the normal-emission photoemission spectra.

3. Results and discussion

Figures 1(a) and (b) show the atomic structures of the reconstructed Si(111)-7 × 7 surface and the Na magic nanocluster on the half unit cell of the 7 × 7 superstructure [9, 26, 27]. The 7 × 7 superstructure is composed of six Si adatoms and three Si restatoms. Figure 1(c) shows the change in the energy distribution curves (EDCs) at the $\bar{\Gamma}$ point with increasing θ_{Na} when Na atoms were adsorbed at RT [26]. The clean Si(111)-7 × 7 surface has three surface states, denoted by S1, S2, and S3, respectively. The S1, S2, and S3 surface states have binding energies of 0.16, 0.84, and 1.7 eV, respectively, and originate from Si adatoms, restatoms, and back-bonds of adatoms, respectively [26]. The S1′ surface state with a binding energy of 0.5 eV comes from

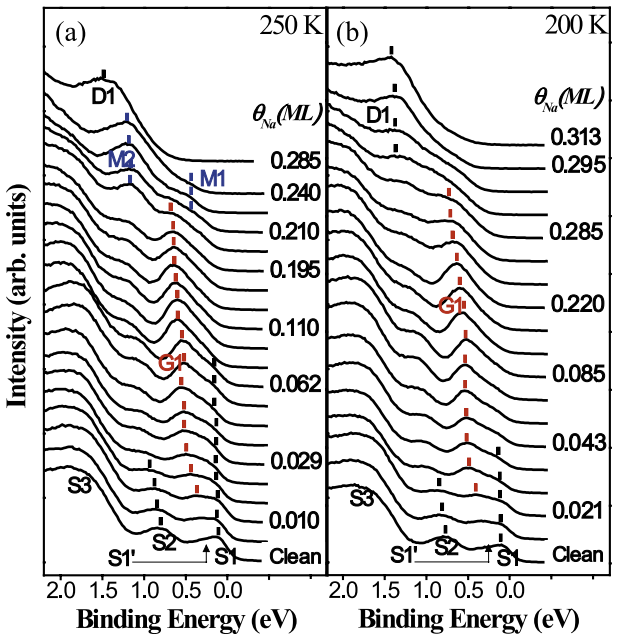

Figure 2. Changes in the PES spectra with increasing θ_{Na} at (a) 250 and (b) 200 K.

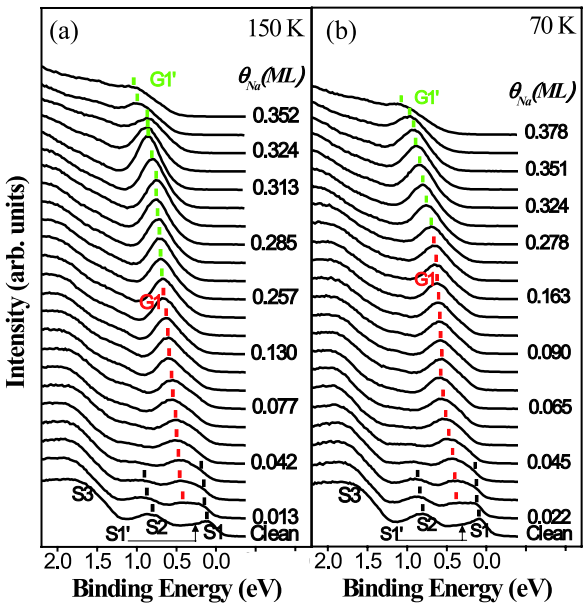

Figure 3. Changes in the PES spectra with increasing θ_{Na} at (a) 150 and (b) 70 K.

adatoms near the corner hole, called corner adatoms [26]. When Na atoms were adsorbed without destroying the overall structure of the 7 × 7 superstructure, they were reported to be in the form of a gas phase below the critical θ_{Na} of 0.08 ML [9, 27]. In the gas phase, Na atoms frequently hop on identical neighboring adsorption sites, where the preferential adsorption site is located between the Si adatom and the restatom [9]. There are three identical adsorption sites around a Si restatom, which is a so-called basin denoted by the yellow circle in figure 1(a), and three basins exist in the half unit cell. Therefore, there are three different hopping mechanisms with different barrier energies: hopping within a single basin, hopping between the basins, and hopping across the border of the half unit cell [27]. The G1 surface state in figure 1(c) originates from the Na atoms in the gas phase and shows a shift from a binding energy of 0.35 eV to a binding energy of 0.6 eV with increasing θ_{Na} [26]. Above the critical θ_{Na}, the gas phase undergoes an irreversible phase transition to a 2D array of identical magic nanoclusters; its atomic structure (figure 1(b)) is composed of six Na atoms and three Si atoms, resulting from Si adatoms being replaced by three Na atoms [9]. The magic nanocluster has two surface states, denoted by M1 (binding energy = 0.45 eV) and M2 (1.1 eV), as shown in figure 1(c) [26]. Above the second critical θ_{Na} of 0.22 ML, the 2D array of the magic nanoclusters irreversibly changes into a disordered phase [28], where the critical θ_{Na} of the phase transition from the gas phase to the 2D array of magic clusters will hereafter be called the first critical θ_{Na}. The disorder phase has a surface state, denoted by D1, with a binding energy of 1.5 eV [26].

To understand the temperature dependence of the RT phase transitions between the three phases, the changes in the EDCs at the $\bar{\Gamma}$ point were acquired at various temperatures. Specifically, Na atoms were adsorbed while cooling the sample at a fixed temperature, and EDCs were measured at the same temperature with increasing θ_{Na}. Figures 2 and 3 show the changes in EDCs at different temperatures of 250, 200, 150, and 70 K. The overall shift of the electronic structure by an external effect such as a surface photovoltage effect was not considered; the binding energies were calibrated by the binding energy of the S3 surface state originating from the back-bonds of the Si adatoms, which are less affected by the phase transitions [26]. At 250 K (figure 2(a)), the G1 surface state began to appear at the same θ_{Na} (0.02 ML) and binding energy (0.35 eV) as those at RT with the gradual disappearance of the S1 and S2 surface states. The G1 surface state persisted up to θ_{Na} of 0.21 ML at 250 K while the G1 surface state at RT existed up to θ_{Na} of 0.09 ML. Furthermore, the binding energy of the G1 surface state shifted to a higher binding energy of 0.65 eV. Above θ_{Na} of 0.22 ML, the M1 and M2 surface states were observed at the same binding energies as those at RT. After the disappearance of the M1 and M2 surface states at θ_{Na} of 0.28 ML, the D1 surface state with the same binding energy as that at RT was observed. Therefore, the number of surface states and their binding energies are very similar to those at RT. This suggests that the 2D gas–nanocluster–disorder phase transition at RT also occurs at 250 K. This is consistent with STM experiments which showed the existence of Na magic nanoclusters below RT [27]. The first critical θ_{Na} of the 2D gas–nanocluster phase transition increased at 250 K compared to that at RT but the second critical θ_{Na} of the 2D nanocluster–disorder phase transition did not change.

Figure 2(b) shows the change in EDCs at 200 K. The G1 surface state, which was observed at 250 K and RT, began to appear at similar θ_{Na} and its binding energy was not much different from those observed at 250 K and RT. The G1 surface state shifted up to a higher binding energy with increasing θ_{Na}, while the S1 and S2 surface states gradually disappeared.

The changes in the S1, S2, and G1 surface states at 200 K are quite similar to those at 250 K and RT. In comparison to the changes, the evolution of the G1 peak at higher θ_{Na} is different from those at 250 K and RT. The G1 surface state persisted up to a higher θ_{Na} of 0.29 ML and its binding energy was saturated at a higher value of 0.7 eV. The change in the G1 surface state suggests that the G1 surface state at 200 K has the same origin as those at 250 K and RT, but its stability as a function of θ_{Na} is different. For this reason, we suggest that the G1 surface state at 200 K also originates from the Na gas phase. After the disappearance of the G1 peak at θ_{Na} of 0.29 ML, a surface state with a binding energy of 1.4 eV, which is similar to the D1 surface states at 250 K and RT, was observed. The θ_{Na}s at which the D1 surface states were observed at 250 K and RT, were similar to that at 200 K. Thus, the surface state was believed to have the same origin and was assigned to D1. On the other hand, the M1 and M2 surface states, which were observed at 250 K and RT, were not found. The nonexistence of the M1 and M2 surface states, which originate from Na magic nanoclusters, suggests that the Na magic nanoclusters do not form at 200 K. Furthermore, because the D1 surface state appears after the disappearance of the G1 surface state, the Na gas phase may undergo a phase transition directly to the disordered phase.

When the sample temperature was further lowered below 150 K, different spectral evolutions were observed, as shown in figure 3. At 150 K (figure 3(a)), the appearance of the G1 surface state, after the disappearance of the S1 and S2 surface states, with increasing θ_{Na} is similar to those at 200, 250 K, and RT. The G1 surface state gradually shifted to a higher binding energy with increasing θ_{Na}, as observed at higher sample temperatures. In comparison to higher sample temperatures, the G1 surface state suggests that the G1 surface state persists up to a high θ_{Na} of 0.35 ML. Furthermore, other surface states, such as the M1, M2, and D1 surface states that were observed at higher sample temperatures, were not found up to θ_{Na} of 0.35 ML. The nonexistence of the M1, M2, and D1 surface states at 150 K suggests that the Na magic nanoclusters, which are the origin of the M1 and M2 surface states, and the disordered phase, which is the origin of the D1 surface state, do not exist at 150 K. When the existence of the G1 surface state at high θ_{Na} is interpreted as it is, the Na gas phase, which produces the G1 surface state, must exist at high θ_{Na} at which a disordered phase is found at higher sample temperatures. However, the existence of the Na gas phase at high θ_{Na} is not reasonable because Na atoms cover most regions of the surface at high θ_{Na} so that there is not enough space to maintain the Na gas phase. On the other hand, the evolution of the EDCs at 70 K (figure 3(b)) is quite similar to that at 150 K. For better understanding of the evolution of the G1 surface state, the changes in the binding energies of the G1 surface states at different sample temperatures were plotted as a function of θ_{Na}, as shown in figure 4(a). The G1 surface states at RT and 250, 200, 150, and 70 K are denoted by black open rectangles, red open circles, green open triangles, blue open triangles, and blue open diamonds, respectively. The black solid rectangle, red solid circle, and green solid triangle indicate the θ_{Na}s at which the G1 surface states disappear at

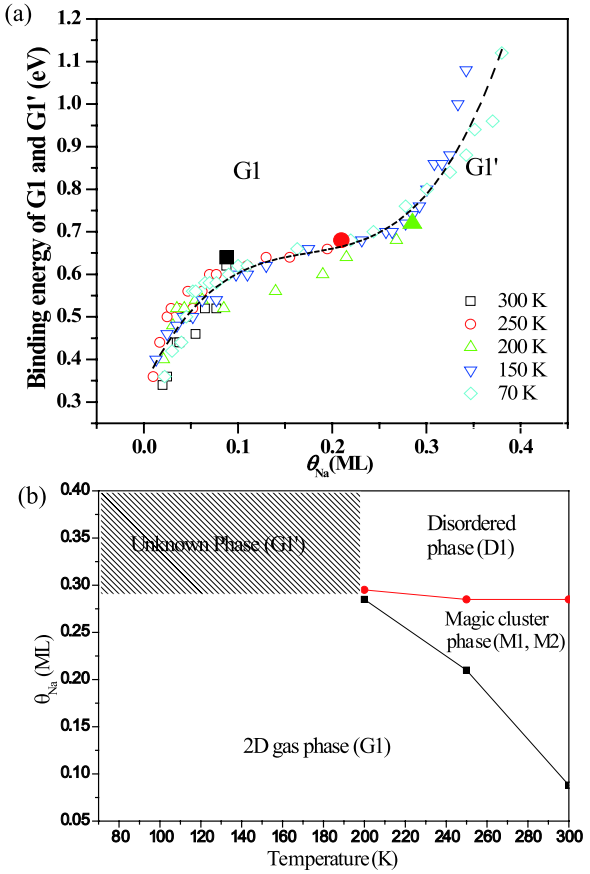

Figure 4. (a) Changes in the binding energies of the G1 and G1′ surface states with increasing θ_{Na} at various temperatures. (b) The phase diagram of sodium atoms as a function of temperature and θ_{Na}, where the black and blue lines denote the first and second critical θ_{Na}s, respectively, and the gray region denotes an unknown phase.

each temperature. Interestingly, the changes in the binding energies of the G1 surface states follow nearly the same curvature and are nearly independent of sample temperatures. The curvature in the plot of the G1 surface states has an inflection point. The existence of the inflection point suggests that the origin of the G1 surface states at lower θ_{Na}s may be different from that at higher θ_{Na}s. This interpretation may be more reasonable because the Na gas phase may not exist at high θ_{Na}s, as discussed above. For this reason, the G1 surface state above 0.28 ML is assigned to the G1′ surface state, as shown in figures 3 and 4(a).

From the characteristic surface states of the phases, the temperature–θ_{Na} phase diagram of the Na-covered Si(111)-7 × 7 surface was determined, as shown in figure 4(b). Here, we note that the phase transitions in the phase diagram are irreversible; for example, the gas phase with lower θ_{Na} can undergo a phase transition to the cluster phase with higher θ_{Na}, but its reversible phase transition is not allowed. In addition, because the characteristic surface states of the different phases coexist within a finite θ_{Na} range, as observed in the PES experiments, the phase boundaries in the phase diagram are not discrete and different phases coexist near the boundaries. The phase boundary indicates the θ_{Na} at

which the surface state of a phase with higher θ_{Na} is clearly observed. As discussed above, the gas–cluster–disorder phase transition occurs at RT with increasing θ_{Na}. The critical θ_{Na} of the gas–cluster phase transition increases with decreasing sample temperature. In comparison to the gas–cluster phase transition, the cluster–disorder phase transition was nearly independent of the sample temperature. The phase diagram suggests that the allowed θ_{Na} range for the magic cluster becomes narrower at a lower sample temperature and the gas phase is relatively more stable at high θ_{Na} at a lower sample temperature. The two critical θ_{Na}s are merged at 200 K and the gas phase undergoes a phase transition directly to the disordered phase. Below 200 K, the gas phase undergoes a phase transition to an unknown phase.

The temperature-dependent diffusion of Na atoms, which was suggested by Wu *et al*, may be related to the phase diagram [27]. Wu *et al* suggested that there are three different diffusion processes, namely diffusion inside the basin (D1 diffusion), diffusion between different basins in the same half unit cell (D2 diffusion), and diffusion across boundaries of the half unit cells (D3 diffusion) [27], where the basin is denoted by the yellow ring in figure 1 and there are three identical basins in the half unit cell. The energy barriers of the D1, D2, and D3 diffusion processes were suggested to be 0.14, 0.36, and 0.42 eV, respectively. Wu *et al* further reported that Na atoms are repulsive to each other in the same basin, but interactions between two Na atoms located at different basins are very weak, resulting in the uniformly distributed 2D Na gas [27]. Based on the diffusion mechanism, the D3 diffusion process is suppressed first with decrease of the sample temperature. At RT, the Na atoms are preferentially adsorbed on the unfaulted half unit cell rather than the faulted half unit cell because of a binding energy difference between the unfaulted and faulted half unit cells of 80 meV [9, 27]. More Na atoms are located at the unfaulted half unit cell at RT, compared to the faulted half unit cell. With decrease of the sample temperature, the D3 diffusion becomes suppressed so that more Na atoms may be located at the faulted half unit cell and fewer Na atoms may be located at the unfaulted half unit cell. This may lead to the result that the number of half unit cells with six Na atoms, which are required to form a magic cluster, is reduced at the same θ_{Na} with decrease of the sample temperature. The higher critical θ_{Na} of the gas–cluster phase transition at a lower sample temperature may originate from the reduced number of Na atoms on the unfaulted half unit cell due to the suppressed D3 diffusion. On the other hand, the six Na atoms need a finite energy to form a magic nanocluster because three Si atoms must be substituted with three Na atoms among the six Na atoms [9, 27]. For this reason, when there is not enough thermal energy for the substitution, Na atoms are just adsorbed on the half unit cell. Therefore, the reason why the magic nanocluster does not form below 200 K, as shown in the phase diagram, may be that the thermal energy is too small to overcome the energy barrier for the substitution.

4. Conclusions

The temperature dependence of the RT gas–cluster–disorder phase transition was studied using PES experiments; this phase transition is irreversible. The gas, cluster, and disordered phases were identified by their specific surface states. The surface state of the gas phase has a binding energy of 0.35 eV at the initial stage and shifts to a higher binding energy with increasing θ_{Na}. The cluster phase has surface states with binding energies of 0.45 and 1.1 eV, respectively. The disordered phase has a surface state with a binding energy of 1.5 eV. With decreasing temperature, the first critical θ_{Na} between the gas and cluster phases increased but the second critical θ_{Na} between the cluster and disordered phases did not change. Subsequently, the two critical θ_{Na}s merged at 200 K. Below 200 K, the gas–cluster–disorder phase transition did not occur and the gas phase underwent a phase transition into an unknown phase. The phase diagram could be understood from the diffusion mechanism of Na atoms, which was suggested by Wu *et al* [27]. Suppressed diffusion of Na atoms across boundaries of half unit cells at a lower sample temperature may be related to the higher critical θ_{Na} of the gas–cluster phase transition. The nonexistence of the cluster phase below 200 K could be ascribed to a low thermal energy that is not enough to overcome the energy barrier for the substitution of Si atoms with Na atoms that is required to form the cluster. For better understanding, further theoretical calculations and experiments will be required in the future, which will contribute to research on 2D diffusion mechanisms such as the lattice gas model [29].

Acknowledgments

This study was supported by the Priority Research Centers Program through the National Research Foundation of Korea (NRF) (2011-0031392) and the National Research Foundation of Korea (NRF) grant funded by the Korea government (MEST) (No. 2012R1A1A2041241) and the Research Center Program of IBS (Institute for Basic Science) in Korea.

References

[1] Ahn J R, Kang P G, Ryang K D and Yeom H W 2005 *Phys. Rev. Lett.* **95** 196402
[2] Crain J N, Kirakosian A, Altmann K N, Bromberger C, Erwin S C, McChesney J L, Lin J L and Himpsel F J 2003 *Phys. Rev. Lett.* **90** 176805
[3] Ahn J R, Byun J H, Koh H, Rotenberg E, Kevan S D and Yeom H W 2004 *Phys. Rev. Lett.* **93** 106401
[4] Ahn J R, Yeom H W, Yoon H S and Lyo I-W 2003 *Phys. Rev. Lett.* **91** 196403
[5] Crain J N, Stiles M D, Stroscio J A and Pierce D T 2006 *Phys. Rev. Lett.* **96** 156801
[6] Erwin S C and Himpsel F J 2010 *Nature Commun.* **1** 58
[7] Nita P, Jalochowski M, Krawiec M and Stepniak A 2011 *Phys. Rev. Lett.* **107** 026101
[8] Li J-L, Jia J-F, Liang X-J, Liu X, Wang J-Z, Xue Q-K, Li Z-Q, Tse J S, Zhang Z and Zhang S B 2002 *Phys. Rev. Lett.* **88** 066101
[9] Wu K *et al* 2003 *Phys. Rev. Lett.* **91** 126101
[10] Li S-C, Jia J-F, Dou R-F, Xue Q-K, Batyrev I G and Zhang S B 2004 *Phys. Rev. Lett.* **93** 116103
[11] Rauscher H, Braun J and Behm R J 2006 *Phys. Rev. Lett.* **96** 116101
[12] Liu H, Chou J-P, Li R-W, Wei C-M and Miki K 2011 *Phys. Rev.* B **83** 075405

[13] Mark A G and McLean A B 2012 *Phys. Rev.* B **85** 195448
[14] Byun J H, Ahn J R, Choi W H, Kang P G and Yeom H W 2008 *Phys. Rev.* B **78** 205314
[15] Johansson L S O and Reihl B 1991 *Phys. Rev. Lett.* **67** 2191
[16] Liebsch A 1991 *Phys. Rev. Lett.* **67** 2585
[17] Fouquet P and Witte G 1999 *Phys. Rev. Lett.* **83** 360
[18] Jeon D, Hashizume T, Sakurai T and Willis R F 1992 *Phys. Rev. Lett.* **69** 1419
[19] Song F and Bergmann G 2002 *Phys. Rev. Lett.* **88** 167202
[20] Magnusson K O and Reihl B 1990 *Phys. Rev.* B **41** 12071
[21] Reihl B, Dudde R, Johannsson L S O, Magnusson K O, Sorensen S L and Wirklund S 1992 *Appl. Surf. Sci.* **56–58** 123
[22] Weitering H H, Chen J, DiNardo N J and Plummer E W 1993 *Phys. Rev.* B **48** 8119
[23] Jostell U 1979 *Surf. Sci.* **82** 333
[24] Aruga T, Tochihara H and Murata Y 1984 *Phys. Rev. Lett.* **53** 372
[25] Tsuei K-D, Plummer E W and Feibelman P J 1989 *Phys. Rev. Lett.* **63** 2256
[26] Ahn J R, Yoo K, Seo J T, Byun J H and Yeom H W 2005 *Phys. Rev.* B **72** 113309
[27] Wu K H *et al* 2004 *Phys. Rev.* B **70** 195417
[28] Hwang C G, Kim N D, Shin S Y, Chung J W, Nam J H, Kim M K, Park C-Y and Ahn J R 2008 *Surf. Sci.* **602** 2300
[29] Rothman D H and Zaleski S 1994 *Rev. Mod. Phys.* **66** 1417